Final Report for Period: 05/2010 - 04/2011   **Submitted on:** 05/31/2011
Principal Investigator: Egedal-Pedersen, Jan .   **Award ID:** 0613734
Organization: MIT
Submitted By:
Egedal-Pedersen, Jan - Principal Investigator
Title:
Laboratory Studies of Spontaneous Reconnection and Intermittent Plasma Objects

Project Participants

Senior Personnel

  Name: Egedal-Pedersen, Jan
  Worked for more than 160 Hours: Yes
  Contribution to Project:

  Name: Porkolab, Miklos
  Worked for more than 160 Hours: Yes
  Contribution to Project:

Post-doc

Graduate Student

Undergraduate Student

Technician, Programmer

Other Participant

Research Experience for Undergraduates

Organizational Partners

Other Collaborators or Contacts

Activities and Findings

Research and Education Activities: (See PDF version submitted by PI at the end of the report)
Please see attached file

Findings:
We have preformed experiments yielding direct evidence of

1. spontaneous magnetic reconnection.
2. 3D effects in the onset of magnetic reconnection.
3. non-linear plasma filament formation and drag by neutral gas.

Training and Development:

Three graduate students and four undergraduate students has been trained on this basic plasma physics experiment. They all acquire experience in building plasma diagnostic, operating the facility, analyzing data and writing publications.

Outreach Activities:

Our main research activities are now documented on the webpage:
http://www.psfc.mit.edu/~jegedal/.

Journal Publications

Katz, N; Egedal, J; Fox, W; Le, A; Porkolab, M, "Experiments on the propagation of plasma filaments", PHYSICAL REVIEW LETTERS, p. , vol. 101, (2008). Published, 10.1103/PhysRevLett.101.01500

Fox, W; Porkolab, M; Egedal, J; Katz, N; Le, A, "Laboratory Observation of Electron Phase-Space Holes during Magnetic Reconnection", PHYSICAL REVIEW LETTERS, p. , vol. 101, (2008). Published, 10.1103/PhysRevLett.101.25500

Le, A; Egedal, J; Daughton, W; Drake, JF; Fox, W; Katz, N, "Magnitude of the Hall fields during magnetic reconnection", GEOPHYSICAL RESEARCH LETTERS, p. , vol. 37, (2010). Published, 10.1029/2009GL04194

Le, A; Egedal, J; Daughton, W; Fox, W; Katz, N, "Equations of State for Collisionless Guide-Field Reconnection", PHYSICAL REVIEW LETTERS, p. , vol. 102, (2009). Published, 10.1103/PhysRevLett.102.08500

Katz, N; Egedal, J; Fox, W; Le, A; Bonde, J; Vrublevskis, A, "Laboratory Observation of Localized Onset of Magnetic Reconnection", PHYSICAL REVIEW LETTERS, p. , vol. 104, (2010). Published, 10.1103/PhysRevLett.104.25500

Egedal, J; Daughton, W; Drake, JF; Katz, N; Le, A, "Formation of a localized acceleration potential during magnetic reconnection with a guide field", PHYSICS OF PLASMAS, p. , vol. 16, (2009). Published, 10.1063/1.313073

Egedal, J; Fox, W; Katz, N; Porkolab, M; Oieroset, M; Lin, RP; Daughton, W; Drake, JF, "Evidence and theory for trapped electrons in guide field magnetotail reconnection", JOURNAL OF GEOPHYSICAL RESEARCH-SPACE PHYSICS, p. , vol. 113, (2008). Published, 10.1029/2008JA01352

Fox, W; Porkolab, M; Egedal, J; Katz, N; Le, A, "Laboratory observations of electron energization and associated lower-hybrid and Trivelpiece-Gould wave turbulence during magnetic reconnection", PHYSICS OF PLASMAS, p. , vol. 17, (2010). Published, 10.1063/1.343521

Egedal, J; Le, A; Zhu, Y; Daughton, W; Oieroset, M; Phan, T; Lin, RP; Eastwood, JP, "Cause of super-thermal electron heating during magnetotail reconnection", GEOPHYSICAL RESEARCH LETTERS, p. , vol. 37, (2010). Published, 10.1029/2010GL04348

Dahlburg, J; Amatucci, W; Brown, M; Chan, V; Chen, J; Cothran, C; Chua, D; Dahlburg, R; Doschek, G; Egedal, J; Forest, C; Howard, R; Huba, J; Ko, YK; Krall, J; Laming, JM; Lin, R; Linton, M; Lukin, V; Murphy, R; Rakowski, C; Socker, D; Tylka, A; Vourlidas, "Exploiting Laboratory and Heliophysics Plasma Synergies", ENERGIES, p. 1014, vol. 3, (2010). Published, 10.3390/en3050101

Egedal, J; Le, A; Katz, N; Chen, LJ; Lefebvre, B; Daughton, W; Fazakerley, A, "Cluster observations of bidirectional beams caused by electron trapping during antiparallel reconnection", JOURNAL OF GEOPHYSICAL RESEARCH-SPACE PHYSICS, p. , vol. 115, (2010). Published, 10.1029/2009JA01465

Ng, J; Egedal, J; Le, A; Daughton, W; Chen, LJ, "Kinetic Structure of the Electron Diffusion Region in Antiparallel Magnetic Reconnection", PHYSICAL REVIEW LETTERS, p. , vol. 106, (2011). Published, 10.1103/PhysRevLett.106.06500

Books or Other One-time Publications

Web/Internet Site

Other Specific Products

Contributions

Contributions within Discipline:

As described above, we have identified spontaneous magnetic reconnection events in VTF. We find that the onset of reconnection is Three-dimensional, which is in contrast to the assumptions applied in most numerical simulation schemes. A Physical Review Letter was recently accepted for publication, detailing a new onset model for reconnection. Also we have derived new equations of state for guide-field reconnection. These equation has been extended to the case without a guide magnetic fields and control the structure of the inner reconnection region (see publications by A. Le et al. and J. Ng et al.)

Contributions to Other Disciplines:

Our recent finding on spontaneous reconnection is acquiring significant interest from scientists working on reconnection in the Earth magnetosphere and the Sun's corona.

Contributions to Human Resource Development:

Contributions to Resources for Research and Education:

Three graduate students and four undergraduate students are being trained in plasma physics on this project.

Contributions Beyond Science and Engineering:

Conference Proceedings

Categories for which nothing is reported:

Organizational Partners

Any Book

Any Web/Internet Site

Any Product

Contributions: To Any Human Resource Development

Contributions: To Any Beyond Science and Engineering

Any Conference

Annual Report for the project "Three-Dimensional Onset and Evolution of Spontaneous Reconnection" Award number: 0844620.

We are happy to report on a very productive year for our group. In total the work, funded in part by the present NSF CAREER award 0844620 and the NSF/DOE award 0613734, has resulted in 9 major publications over the past year [1-9] including two publications by graduate students in Physical Review Letters [2,6]. In our original budgets we included the cost of a Post-Doc, however the necessary funding was not made available and a Post-Doc was not hired. The funding we did obtain from the two grants above has covered the cost of maintaining the experiment, three graduate students as well as the cost for publishing their vast achievements in peer reviewed journals.

First we summarize the results of our recent experimental investigations in the Versatile Toroidal Facility (VTF). The details of our earlier experimental and theoretical findings are documented in seven Physical Review Letters [10-16] and several other journal papers [17-25]. At the end we have appended slides highlighting the various research topics.

Our reconnection experiments are based on a recently developed magnetic geometry including four co-axial coils. The picture in Figure 1(Left) shows these coils during their installation. As illustrated on the RHS diagram, the coils implement a new reconnection drive scenario, where reconnection is driven by transferring the coil current from the center loops to the outer loops.
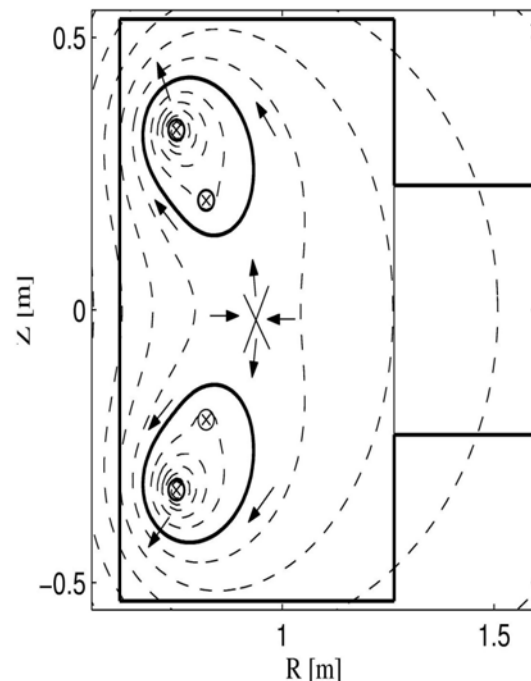
Figure 1. Left: Installation of internal coils implementing a new magnetic geometry. Right: Illustration of the new reconnection drive scenario applied in VTF. This geometry includes spontaneous reconnection events where the reconnection rate at first is slow and then suddenly transitions into a burst of fast reconnection. The bulk of our work for the past year has been focused on the construction of new magnetic arrays to measure possible 3D effects in the onset of spontaneous reconnection. In experimental configurations where the plasma dynamics is reproducible, magnetic data can be collected in multiple discharges and combined to provide spatially resolved profiles of the plasma dynamics. However, to investigate spontaneous reconnection where the reconnection process is not reproducible all information on the plasma must be collected in a single discharge. Our newly developed magnetic flux arrays measure directly the toroidal component of the magnetic vector potential. From this quantity, the magnetic field geometry, current density, and reconnection rate are readily obtained. The details of our new approach to measure the magnetic properties during reconnection are described in Review of Scientific Instruments [24].
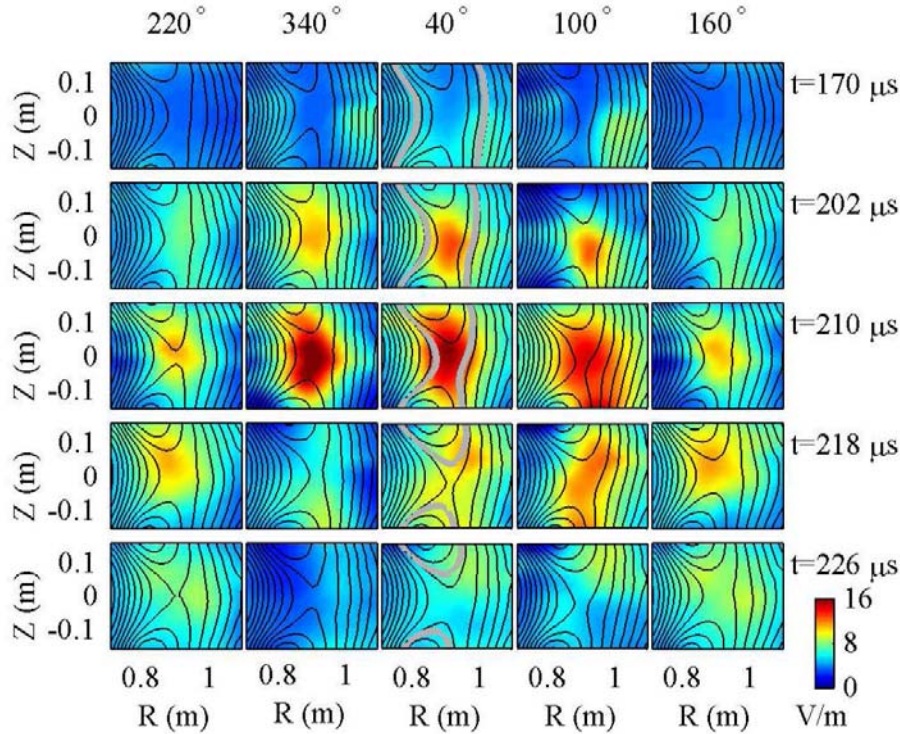

Figure 2. Poloidal cross-sections of $\partial A_\varphi/\partial t$ for different toroidal angles and times. The onset angle is $\varphi = 0\circ$, and the peak reconnection rate occurs at $t = 210$ μs. Superimposed is the poloidal projection of magnetic field lines, one of which at $\varphi = 40\circ$ is followed in gray. By $t = 218$ μs, $\partial A_\varphi/\partial t$ has propagated to the far side of the torus ($\varphi = 160\circ$).

Our most recent experiments document how the onset phase of reconnection involves strong three-dimensional dynamics. The reconnection starts a one toroidal location, and then propagates around the toroidal direction at about the Alfven speed. The three

dimensional measurements include the detailed time evolution of the plasma density, current density, the magnetic flux function, the electrostatic potential and the reconnection rate. As an example of the 3D dynamics in Fig. 2 we show measurements of $\partial A_\varphi/\partial t$ for different toroidal angles and times. It is clearly seen how reconnection starts at one toroidal angle and then propagates around the device. A Physical Review Letter is now published [6] that characterizes the details of the onset of reconnection and provides a new model for the onset dynamics which accurately reproduces the initial growth rate of the events. Additional details on our spontaneous reconnection event will be published in a paper submitted to Physics of Plasmas [9].

We have also characterized fast fluctuations during the spontaneous reconnection events. Significantly elevated fluctuations are observed during these events including frequencies all the way up the electron cyclotron frequency. The analysis of this has been reported in William Fox's PhD thesis in the spring of 2009. The results of this work will also be detailed in a recent publication in Physic of Plasmas [8].

Previous experiments on VTF utilized an open cusp configuration where the magnetic field lines intersect the walls of the vacuum vessel. Our theoretical understanding of reconnection in this configuration was fundamental for interpreting recent in situ measurements (by the Wind spacecraft) of the electron phase space distribution function during reconnection in the deep magnetotail. Based on the electron distributions measured by Wind we showed that electrons are trapped inside the reconnection region during magnetotail reconnection [13]. This result, recently confirmed in numerical simulations [25, 2, 4, 5], has significant implications for the reconnection rate because trapping reduces the free streaming of electrons along magnetic field lines. This is important because theory predicts that a local decrease in conductivity can cause fast reconnection.
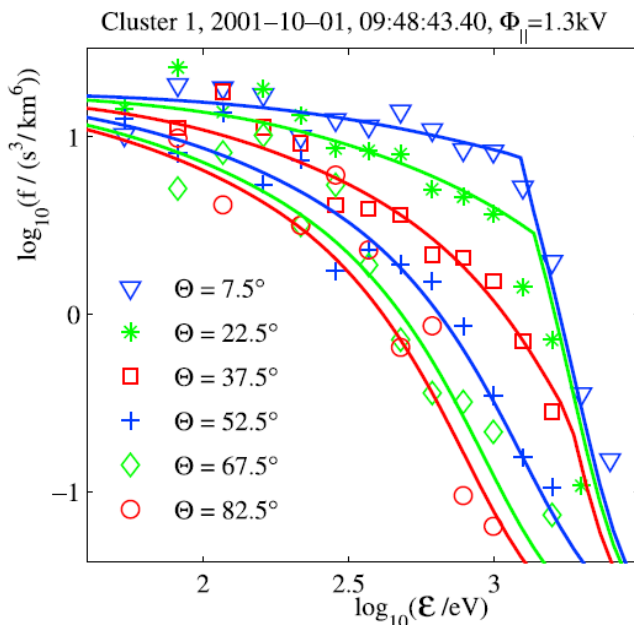

Figure 3: Detailed comparison between the model electron distribution in Ref. [3] and the electron distribution measured by Cluster 1 on 1 October 2001 at 0948:43.40.

Our most recent work shows that in reconnection events observed by the Cluster mission electrons become trapped in positive potential structures ranging up to 20kV [3]. As illustrated in Fig. 3 the model developed on the basis of VTF observations is in excellent agreement with the measurements by the Cluster mission of the electrons in a reconnection inflow region.

Furthermore, by analyzing spacecraft data we find that the parallel electric fields associated with electron trapping are likely the main cause of electron energization in the Earth's magnetotail. This has been documented in a recent Geophysical Research Letter [7]. As an example, in Fig.4 we have included a comparison between our model for the energy gain of the super-thermal electrons and in-situ observations by the Wind spacecraft.
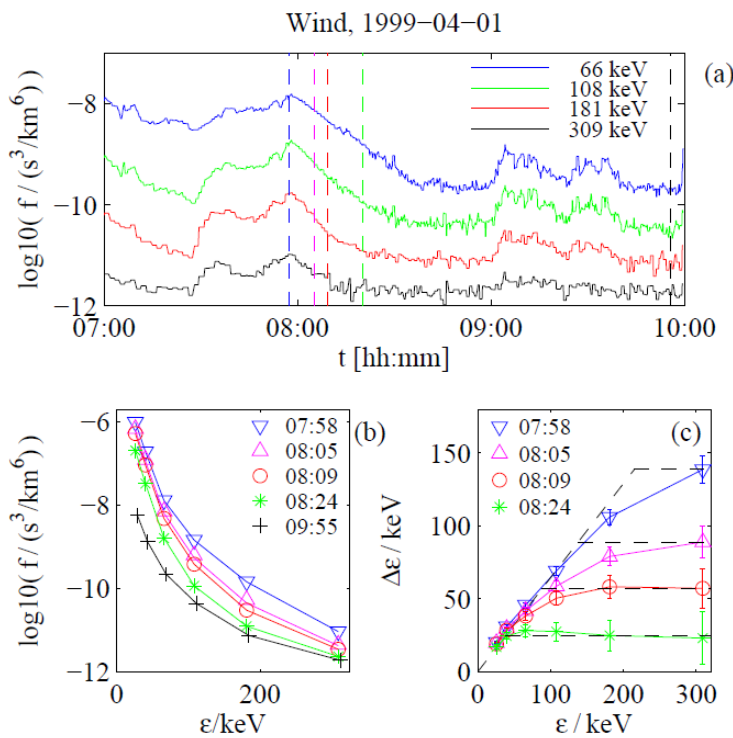

Figure 4: (a) Electron phase-space densities from the Wind spacecraft. (b) Electron distribution observed at separate time points (the data is average over two minutes to reduce noise). The data at t = 09:55 is the lobe distribution of incoming electrons. (c) Spectra of the electron energy gain for four separate points in time. The dashed lines are obtained with the model developed in Ref [7].
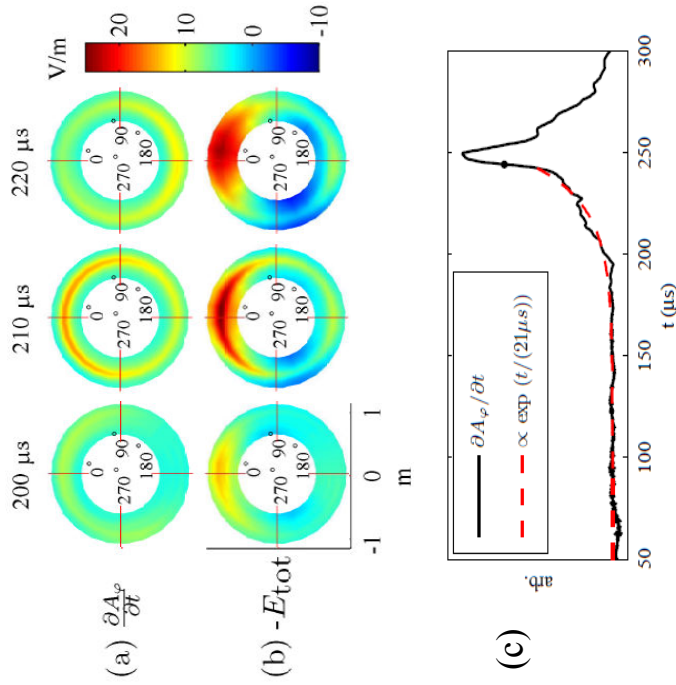
Sincerely *Jan Egedal*

Dr. Jan Egedal

References. (publications related to the work over the past year are in bold).

[1] Egedal J, Daughton W, Drake J F, Katz N, Le A, "Formation of a localized acceleration potential during magnetic reconnection with a guide field.", (2009) Physics of Plasmas 16, 050701.

[2] Le A, Egedal J, Daughton W, Fox W, Katz N, "The Equations of State for Collisionless Guide-Field Reconnection", (2009) Phys. Rev. Lett. 102, 085001.

[3] Egedal J, Le A, Katz A, Chen L-J, Lefebvre B, and Daughton W, "Cluster Observations of Bi-directional Beams Caused by Electron Trapping During Anti-parallel Reconnection", (2010) J. Geophys. Res., 115, A03214.

[4] Le A, Egedal J, Daughton W, Drake J, Fox W, Katz N, "Magnitude of the Hall Fields during magnetic reconnection", (2010) Geophys. Res. Lett. 37, L03106.

[5] Le A, Egedal J, Fox W, Katz N, Vrublevskis A, Daughton W, and Drake J, "Equations of state in collisionless magnetic reconnection", (2010) Physics of Plasmas 17, 055703.

[6] Katz N, Egedal J, Fox W, Le A, Bonde J, and Vrublevskis A, "Laboratory Observation of Localized Onset of Magnetic Reconnection", (2010) Phys. Rev. Lett. 104, 255004.

[7] Egedal J, Le A, Zhu Y, Daughton W, Oieroset M, Phan T, Lin P, Eastwood J, "Cause of Super-thermal Electron Heating during Magnetotail Reconnection", (2010) Geophys. Res. Lett. 37, L10102.

[8] Fox W, Porkolab M, Egedal J, Katz N, and Le A, "Laboratory observations of electron energization and associated lower-hybrid and Trivelpiece-Gould wave turbulence during magnetic reconnection", (2010) Physics of Plasmas 17, 072303.

[9] Katz N, Egedal J, Fox W, Le A, Bonde J, and Vrublevskis A, "Experimental Investigation of the Trigger Problem in Magnetic Reconnection", (2010) submitted for publication in Physics of Plasmas.

[10] J. Egedal and A. Fasoli. Single-particle dynamics in collisionless magnetic reconnection. Phys. Rev. Lett., 86(22):5047–5050, MAY 28 2001.

[11] J. Egedal, A. Fasoli, and J. Nazemi. Dynamical plasma response during driven magnetic reconnection. Phys. Rev. Lett., 90(13):135003, APR 4 2003.

[12] A. Stark, W. Fox, J. Egedal, O. Grulke, and T. Klinger. Laser-induced fluorescence measurement of the ion-energy-distribution function in a collisionless reconnection experiment. Phys. Rev. Lett., 95(23):235005, DEC 2 2005.

[13] J. Egedal, M. Oieroset, W. Fox, and Lin R. P. In situ discovery of an electrostatic potential, trapping electrons and mediating fast reconnection in the earth's magnetotail. Phys. Rev. Lett., 94(2):025006, JAN 21 2005.

[14] J. Egedal, W. Fox, N. Katz, M. Porkolab, K. Reim, and E. Zhang. Laboratory observations of spontaneous magnetic reconnection. Phys. Rev. Lett., 98(1):015003, JAN 5 2007.

[15] N. Katz, J. Egedal, W. Fox, et al. Experiments on the propagation of plasma filaments. Phys. Rev. Lett., 101, 2008.

[16] W. Fox, M. Porkolab, J. Egedal, N. Katz, and A. Le. Laboratory Observation of Electron Phase-Space Holes during Magnetic Reconnection. Phys. Rev. Lett., 101(25), DEC 19 2008.

[17] J. Egedal, A. Fasoli, M. Porkolab, and D. Tarkowski. Plasma generation and confinement in a toroidal magnetic cusp. Review of Scientific Instruments, 71(9):3351–3361, SEP 2000.

[18] J. Egedal, A. Fasoli, D. Tarkowski, and A. Scarabosio. Collisionless magnetic reconnection in a toroidal cusp. Phys. Plasmas, 8(5, Part 2):1935–1943, MAY 2001.

[19] J. Egedal and A. Fasoli. The topology of guiding center orbits in a linear magnetic cusp. Phys. Plasmas, 8(9):4042–4052, SEP 2001.

[20] J. Egedal. A drift kinetic approach to stationary collisionless magnetic reconnection in an open cusp plasma. Phys. Plasmas, 9(4):1095–1103, APR 2002.

[21] J. Egedal, W. Fox, M. Porkolab, and A. Fasoli. Experimental evidence of fast reconnection via trapped electron motion. Phys. Plasmas, 11(5):2844–2851, 2004.

[22] J. Egedal, W. Fox, E. Belonohy, and M. Porkolab. Kinetic simulation of the vtf magnetic reconnection experiment. Computer Physics Communications, 164(1-3):29–33, DEC 1 2004.

[23] J. Egedal, W. Fox, M. Porkolab, and A. Fasoli. Eigenmode response to driven magnetic reconnection in a collisionless plasma. Phys. Plasmas, 12(5):052107, MAY 2005.

[24] A. Kesich, J. Bonde, J. Egedal, et al. Magnetic flux array for spontaneous magnetic reconnection experiments. Review of Scientific Instruments, 79, 2008.

[25] J. Egedal, W. Fox, N. Katz, M. Porkolab, M. Oieroset, R. P. Lin, W. Daughton, and Drake J. F. Evidence and theory for trapped electrons in guide field magnetotail reconnection. J. Geophys. Res., 113(6):A12207, MAR 25 2008.

Observations and model for 3D spontaneous magnetic reconnection

Reconnection events on the sun, in the Earth's magnetotail and in magnetic fusion devices often occurs in spontaneous burst. Reconnection is at first slow which allow for magnetic energy to accumulate in the system. The stored energy is then released in powerful burst of fast reconnection. What causes the change from slow to fast reconnection is still purely understood and the so-called "trigger problem" remains unresolved.
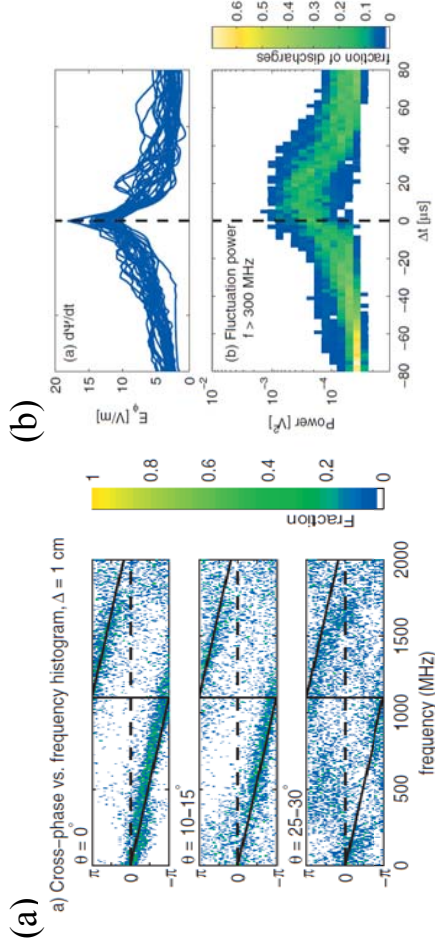
The main experimental focus in the Versatile Toroidal Facility (VTF) at MIT is this trigger problem. The dynamics of powerful spontaneous reconnection events observed in our device have provided a unique opportunity for making progress in this area [1]. Our most recent experiments document how the onset phase of fast reconnection involves strong three-dimensional dynamics. The reconnection starts a one toroidal location, and then propagates around the toroidal direction at about the Alfven speed. The three dimensional measurements include the detailed time evolution of the plasma density, current density, the magnetic flux function, the electrostatic potential and the reconnection rate.

As an example of the 3D dynamics in the figure we show measurements of the reconnection rate, $-\partial A_\phi/\partial t$, as measured at the mid-plane of VTF for different times. It is clearly seen how reconnection starts at one toroidal angle and then propagates around the device. A Physical Review Letter was recently published [2] which characterizes the details of the onset of reconnection and provides a new model for the onset dynamics. The model accurately reproduces the initial growth rate of the events. In addition, Noam Katz (who recently obtained his PhD based on this work) has been awarded an invited talk at the upcoming 52nd APS DPP meeting in Chicago, Nov, 2010.

[1] Egedal J, et al., (2007) Phys. Rev. Lett. 98, 015003.

[2] Katz N, et al., (2010) Phys. Rev. Lett. 104, 255004.

(a) $\frac{\partial A_\varphi}{\partial t}$ 200 μs   210 μs   220 μs

(b) $-E_{\text{tot}}$

(c)

(a) The reconnection rate $-\partial A_\phi/\partial t$, at $Z = 0$ viewed from above; reconnection onset occurs at $\varphi \simeq 0°$ and propagates to $\varphi \simeq 180°$ in about 5-10μs.

(b) The total electric field $E_{\text{tot}} = -\partial A_\phi/\partial t, -\nabla\phi$ remains localized throughout.

(c) Based on the 3D observations a model has been developed which accurately predict the observed grows-rate of the reconnection pulses. The model is now published in PRL .

Observations of turbulence and fast electrons driven by spontaneous magnetic reconnection

(a)

a) Cross-phase vs. frequency histogram, Δ = 1 cm

θ = 0°

θ = 10–15°

θ = 25–30°

frequency (MHz)

Fraction

(b)

(a) dψ/dt

E_ϕ [V/m]

(b) Fluctuation power
f > 300 MHz

Power [V^2]

Δt [μs]

fraction of discharges

(a) Phase measurements for various separations of electrostatic probes. Probes are aligned parallel to the magnetic field. The probes are digitized by a fast oscilloscope rented from Textronix. Coherent Trivelpiece–Gould wave turbulence is observed over a frequency regime 0 - 2 GHz.

(b) Color histogram indicating time correlation of reconnection electric fields and high-frequency fluctuation observations in the Trivelpiece–Gould regime. The observed turbulence is likely driven by a population of fast electrons generated by reconnection.

The starting point for much reconnection study is the Sweet–Parker reconnection framework, which describes steady state reconnection through an extended current sheet. The small aspect ratio of a Sweet–Parker current sheet throttles the mass flow, and this geometrical effect is the major reason why Sweet–Parker reconnection is so slow. However, reconnection simulations employing an ad hoc anomalous resistivity can achieve fast reconnection. A central questions in magnetic reconnection research therefore revolve around the role of turbulence for generating anomalous resistivity.

The observed time-variation of the reconnection rate in VTF is very useful for experimentally discerning which mechanisms influences the reconnection process. As such, a series of experiments has been conducted on the role of turbulence during the magnetic reconnection process. The electrostatic fluctuations are observed by small, high-bandwidth, and impedance-matched Langmuir probes. The observed modes, identified by their characteristic frequency and wavelength, include lower-hybrid fluctuations and high-frequency Trivelpiece–Gould modes. The observed waves are believed to arise from electrons energized by the reconnection process via direct bump-on-tail instability or gradients in the fast electron population lower-hybrid. It is still unclear if the turbulence is strong enough to impact the reconnection rate. The results of the study were recently published in Physics of Plasmas [3].

[3] Fox W, et al., (2010) Physics of Plasmas 17, 072303.

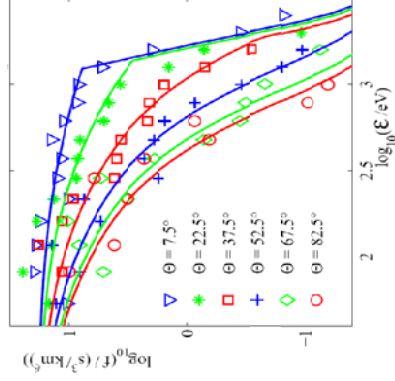# New model for the distribution function of adiabatic electrons during reconnection

Graphical representation of the new adiabatic electron model
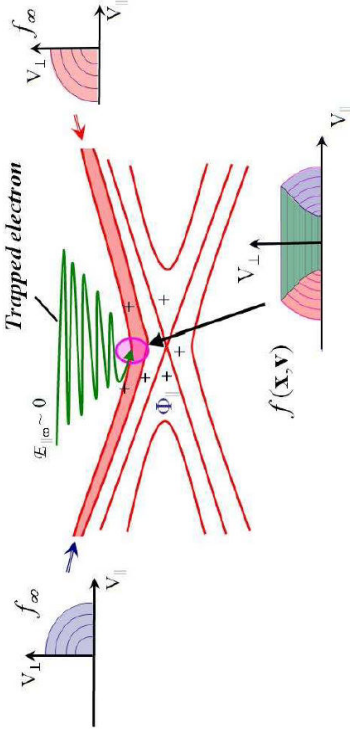
The new expression derived for the electron distribution function

$$f(\mathbf{x}_0, \mathbf{v}_0) = \begin{cases} f_\infty(\mu B_\infty) & , \quad \text{trapped} \\ f_\infty(\mathcal{E}(\mathbf{x}_0) - e\Phi_\parallel(\mathbf{x}_0)) & , \quad \text{passing} \end{cases}$$

The model is consistent with Cluster spacecraft observation

In reconnection, the parallel electric field is proportional to the reconnection rate. To support such an electric field, and hence reconnection, the electron pressure is important for the electron momentum balance. Standard fluid models and simulation schemes often rely on isothermal or adiabatic equations of state for a fluid closure. Meanwhile, measurements taken by the Wind and Cluster spacecraft in reconnecting current sheets in the Earth's magnetotail show that the electron phase space density is highly anisotropic, with $T_\parallel >> T_\perp$. Similar pressure anisotropy is observed in fully kinetic reconnection simulations.

Recently, Egedal et al. introduced a mechanism that accounts for the electron pressure anisotropy [4]. The model is based on a simple solution to the Vlasov equation using conserved quantities of the electron motion in reconnecting current sheets. The model has now been benched marked directly against detailed electron measurements obtained by the Cluster spacecraft mission [5].

[4] Egedal J, et al., (2008) J. Geophys. Res., 113, A12207.

[5] Egedal J, et al., (2010) J. Geophys. Res., 115, A03214.

Equations of State for reconnection providing separate expression for the parallel and perpendicular electron pressures.

As mentioned above, direct in situ observation of magnetic reconnection in the Earth's magnetotail as well as kinetic numerical studies have recently shown that the electron pressure in a collisionless reconnection region is strongly anisotropic. This anisotropy is mainly caused by the trapping of electrons in parallel electric fields. This anisotropy is characterized by the electron model of Egedal et al., 2008 (see [4] above).

Using the new electron model as a starting point, A. Le, et al. [6] derived the Equations of State for the parallel and perpendicular pressures of magnetized electrons. These equations allow a fluid description in a collisionless regime where parallel electric fields and the dynamics of both passing and trapped electrons are essential.

The Equations of State have been tested directly against state-of-the-art kinetic simulations. As shown in the figure, excellent agreement is found between the model and the simulations. The Equations of State are suitable for implementation in two-fluid codes and could be combined with a microscopic dissipation mechanism in the immediate vicinity of the x line (such as hyper resistivity) to investigate large-scale reconnection geometries. This fluid closure is also useful for modeling and interpreting measurements from low-collisionality plasmas in space when a fully kinetic treatment is intractable.

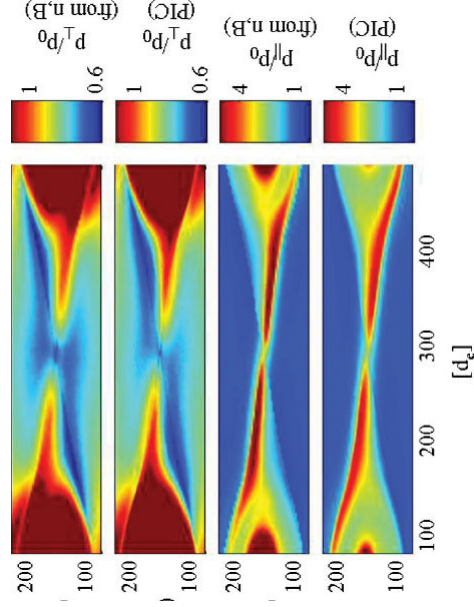The newly derived expressions for the electron pressure components

$$\tilde{p}_\parallel = F(\alpha/2) \times \tilde{n} + F(\alpha^{-1}/2)\frac{\pi \tilde{n}^3}{6\tilde{B}^2},$$

$$\tilde{p}_\perp = F(\alpha)\tilde{n} + F(\alpha^{-1})\tilde{n}\,\tilde{B},$$

where $\tilde{n} = n/n_\infty$, $\tilde{B} = B/B_\infty$, $\tilde{p}_\parallel = p_\parallel/p_\infty$, $\tilde{p}_\perp = p_\perp/p_\infty$, $\alpha = \tilde{n}^3/\tilde{B}^2$, and $F(x) = (1+x)^{-1}$

The new Equations of State are here tested directly against a fully kinetic (PIC) simulation.

Excellent agreement is observed between the simulation and the model

$p_\perp/p_0$ (from n,B)

$p_\perp/p_0$ (PIC)

$p_\parallel/p_0$ (from n,B)

$p_\parallel/p_0$ (PIC)

[d_e]

[6] Le A, et al., (2009) Phys. Rev. Lett. 102, 085001.

# Magnitude of the Hall fields during anti-parallel magnetic reconnection

The figure (based on a kinetic simulation) shows a typical trajectory of a trapped electron in anti parallel reconnection overlaid on contours of constant |B|. In the in the inflow region the electron magnetic moment is conserved and the Equations of State are valid.
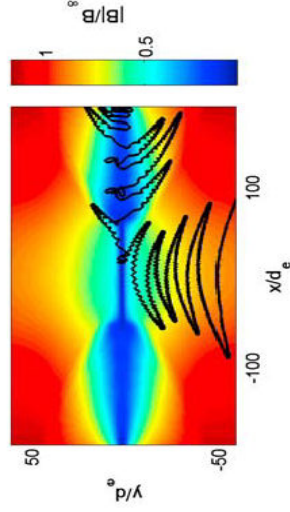
In (a) we consider a vertical cut though the reconnection layer and document how the pressure anisotropy controls the structure and the strength of the electron outflow jets responsible for the Hall magnetic fields.

(b-d) Various scaling laws for the reconnection region has been confirmed using kinetic simulations results provided by D. Daughton

and J. F. Drake. The upstream electron pressure normalized to the magnetic field pressure, $\beta_{e\infty}$, is identified as the parameter controlling the structure of the reconnection region.
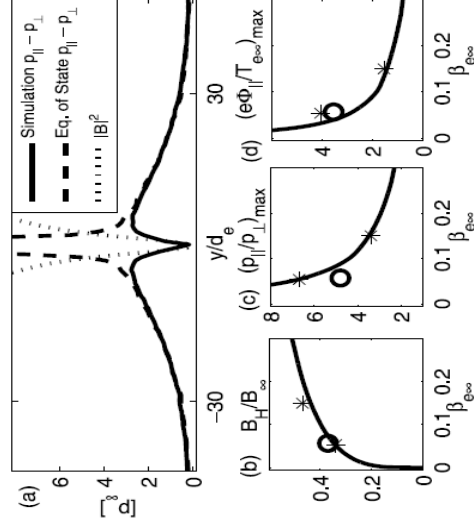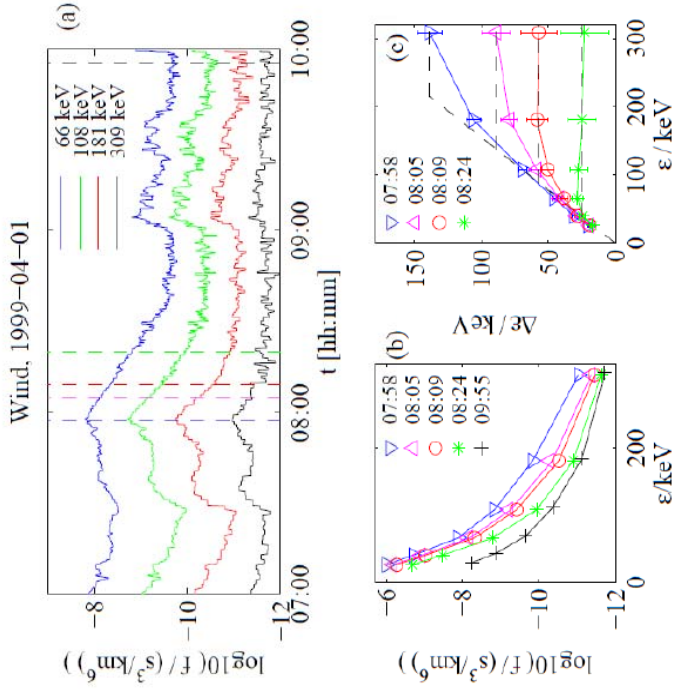

In anti-parallel reconnection, the initial magnetic field geometry contains a neutral sheet where the field vanishes. A striking feature of the inner electron diffusion region observed in kinetic simulations is an extended electron outflow jet. The current carried by this jet generates a signature quadrupolar Hall magnetic field which has been observed in both space data and laboratory experiments. So far there has been no self consistent theory describing the magnitude, B_H, of the Hall fields.

Recently A. Le, et al. showed that the pressure anisotropy in the inflow region is consistent with our new Equations of State up to the narrow layer where our model breaks down. Nevertheless, our model imposes useful relationships between the upstream electron pressure and the Hall magnetic fields just outside the electron layer. By considering force balance of the outflow layer new scaling laws have been derived which predict fundamental quantities for the reconnection electron layer. These scaling laws have been confirmed in fully kinetic simulation [7,8]. This work also resulted in an invited talk for Ari Le at the 51st APS DPP meeting in Atlanta, Nov., 2009.

[7] Le A, et al., (2010) Geophys. Res. Lett. 37, L03106

[8] Le A, et al., (2010) Physics of Plasmas 17, 055703

Cause of Super-thermal Electron Heating during Magnetotail Reconnection

In reconnection events associated with solar flares up to 50% of the released magnetic energy can be converted into kinetic energy of super-thermal (10–100 keV) electrons. In the Earth's magnetotail reconnection is observed to cause electron acceleration up to 300 keV. Electron energization is also fundamentally important to astrophysics because the X-rays generated by super-thermal electrons provide an important window into astrophysical processes. Despite its importance the mechanism that energizes the super-thermal electrons is still not understood.

A recent theoretical study shows that Fermi acceleration of electrons in contracting magnetic islands can produce power-law distributions [Drake et al., *Nature*, 2006] seemingly consistent with those observed in the Earth's magnetotail [Øieroset et al., *PRL*, 2002]. However, we have consider the reconnection event investigated by Øieroset (and another event observed by the Cluster mission). We find that the electron energization, does not obey the scaling law that is the signature of the Fermi acceleration process. Rather, for each event, the spectra of the electron energization are consistent with energization in an acceleration potentials, related to the parallel electric fields in the vicinity of the reconnection regions [9]. Our analysis was recently published in Geophysical Review Letters [10].

[9] Egedal J, et al., (2009) Physics of Plasmas 16, 050701.

[10] Egedal J, et al., (2010) Geophys. Res. Lett. 37, L10102.

(a) Electron phase-space densities of super-thermal electrons measured by the Wind spacecraft during a reconnection event in the deep magnetotail. (b) Electron distribution observed at separate time points (the data is average over two minutes to reduce noise). The data at t = 09:55 is the lobe distribution of incoming electrons. (c) Spectra of the electron energy gain for four separate points in time. The dashed lines are obtained with the model developed in Ref [10] based on acceleration in a parallel potential.

June 2, 2010

Professor Jan Egedal-Pedersen
Department of Physics

Dear Professor Egedal-Pedersen:

I write to inform you that the President and the Executive
Committee of the Corporation have approved your promotion to
Associate Professor, effective July 1, 2010, with an increase in
your salary to $ for the academic year 2010-2011.

Sincerely yours,

Marc A. Kastner
Dean of the School
of Science

Final Report for "Laboratory Studies of Spontaneous Reconnection and Intermittent Plasma Objects",

Award Number: 0613734,

PI: Jan Egedal

MIT Plasma Science and Fusion Center,

Cambridge, MA, 02139

1 Executive summary

The NSF/DOE award No. 0613734, supported two graduate students (now Drs. W. Fox and N. Katz) and material expenses. The grant enabled these students to operate of a basic plasma physics experiment (on magnetic reconnection) at the MIT Plasma Science and Fusion Center and the MIT Physics Department. The study of the collisionless magnetic reconnection constituted the primary work carried out under this grant. The investigations utilized two magnetic configurations with distinct boundary conditions. Both configurations were based upon the Versatile Toroidal Facility (VTF). The first configuration is characterized by open boundary conditions where the magnetic field lines interface directly with the vacuum vessel walls. The reconnection dynamics for this configuration has been methodically characterized and it has been shown that kinetic effects related to trapped electron trajectories are responsible for the high rates of reconnection observed. This type of reconnection has not been investigated before. Nevertheless, the results are directly relevant to observations by the Wind spacecraft of fast reconnection deep in the Earth magnetotail [1]. The second configuration was developed to be relevant to specifically to numerical simulations of magnetic reconnection, allowing the magnetic field-lines to be contained inside the device. The configuration is compatible with the presence of large current sheets in the reconnection region and reconnection is observed in fast powerful bursts. These reconnection events facilitate the first experimental investigations of the physics governing the spontaneous onset of fast reconnection [2]. In this Report we review the general motivation of this work and provide an overview of our experimental and theoretical results enabled by the support through the awards. The details of the individual sections are naturally contained in the relevant publications, indicated in the reference list and annexed to this Report.

2 Introduction

Magnetic reconnection [3] is a fundamental process in plasmas that converts magnetic energy into particle energy while changing the topology of the magnetic field lines. Although reconnection occurs in microscopic diffusion regions it often governs the macro-

scopic properties and behavior of the system. It controls the evolution of explosive events such as solar flares, coronal mass ejections, and magnetic storms in the Earth's magnetotail. The latter drive the auroral phenomena [4, 5, 6, 7]. In magnetic fusion devices magnetic reconnection is responsible for the periodically occurring internal relaxation events (sawtooth reconnection) which can degrade the plasma confinement [8, 9].

Theoretical investigations have mostly concentrated on understanding the steady state of fast reconnection, and it is now widely believed that two-fluid and kinetic effects give rise to the fast time scales of reconnection observed in nature [10, 11, 12]. However, reconnection as observed in nature is explosive, implying that reconnection must be able to transition from slow to fast; the system must be able to accumulate magnetic stress slowly (in the form of a current sheet), then release it quickly. This "trigger problem", the question of what process causes the spontaneous transition from slow to fast reconnection is still not well understood. While direct observations of coronal mass ejections on the sun and sawtooth reconnection in tokamaks indicate that three dimensional effects are important, theoretical investigations of the trigger problem have so far been limited to two dimensional geometries [13, 14, 15, 16].

Three dimensional effects are observed in the onset of reconnection on the sun [17, 18], where a comprehensive analysis of flares seen by the TRACE and SoHo satellites shows that a localized brightening can propagate along an arcade of post-flare loops. As the flare propagates, the flare ribbons at the foot of the loops move apart as well. On MST, Choi et al. [19] found that small sawtooth events are linearly unstable and hence spontaneous, while larger events require a nonlinear mode coupling for the instability to grow. In sawtooth reconnection, detailed measurements by Park et al. [9, 20, 21] and Munsat et al. [22] from the TEXTOR tokamak found toroidally localization of the reconnection events, with reconnection starting at specific toroidal locations with both "good" and "bad" curvature. These observations show that the 2D theories may not capture the essential physics to describe the onset of spontaneous reconnection.

In this report we explore driven and spontaneous reconnection through experimental observations in the Versatile Toroidal Facility (VTF) located at MIT. VTF is a basic plasma physics experiment that allows for probing of the internal plasma parameters. In particular we document the behavior of reconnection in two distinct experimental geometries. In the first geometry the reconnection process is axisymmetric and oscillatory in time, whereas in the second configuration reconnection is three-dimensional an spontaneous, so that the rate grows exponentially. We find that the vastly different behavior can be accounted for in a simple theoretical framework, which is described below. We provide a short overview of the experimental results and focus on the key physics issues related to how breaking the nominal 2D symmetry allows spontaneous reconnection to occur in the experiment. Furthermore, for the experiments where 2D symmetry is maintained we find that electron trapping is fundamentally important in explaining the observations. These trapping effects observed in the experiment are also important to magnetotail reconnection and numerical simulations. Thus, due to the generic importance of electron trapping in reconnection we provide a summary of this work. The present report only seeks to provide an overview of our previous published observations and illustrate their commonalities by applying the same mathematical analysis to our different experimental geometries. More in-depth analysis of the detailed experimental results can be found in the various references provided in the text.

The report is organized as follows. In Section 3 we discuss the observations of 2D reconnection and account for the oscillatory behavior with a simple theoretical framework. In the following section this framework is amended and applied to spontaneous 3D reconnection events. Finally, in Section 5 the report is concluded.

3 Experimental observations of 2D oscillatory reconnection

In Fig. 1 we show the two distinct magnetic configurations applied in the VTF for the study of reconnection. In the open cusp configuration depicted in Fig. 1(a) the in-plane (poloidal) magnetic field is produced by conductors external to the vacuum vessel, such that the magnetic field lines intersect the vacuum vessel. For the closed cusp configuration in Fig. 1(b) the poloidal field is produced by in-vessel coils and the magnetic field lines close inside the experiment yielding improved plasma confinement. Both configurations include a strong toroidal magnetic field produced by a set of toroidal field-coils.

Again, the two configurations exhibit vastly different reconnection dynamics. In the open configuration the reconnection dynamics are toroidally symmetric (2D reconnection) and often oscillatory in time. Meanwhile, in the closed configuration regimes exist where reconnection occurs in powerful bursts characterized by strong toroidal asymmetry (3D reconnection) and by an initial exponential growth in the reconnection rate. We first focus on the more simple 2D reconnection dynamics observed in the open configuration.
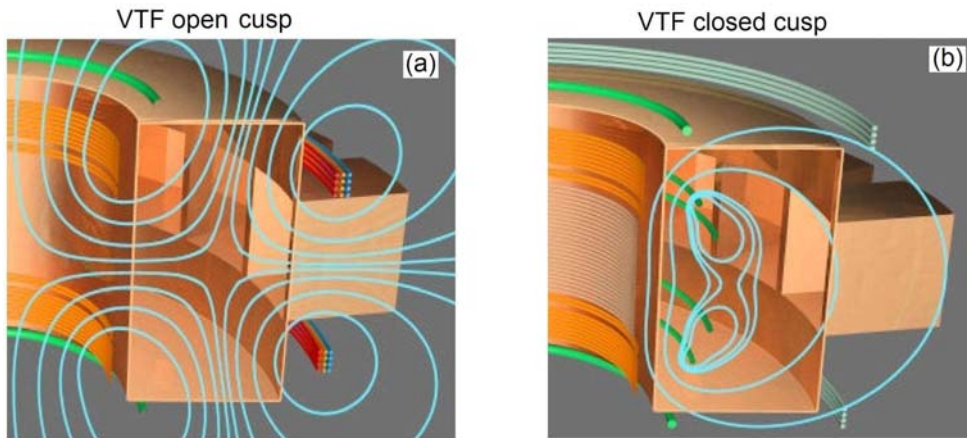

Figure 1: Illustration of the poloidal magnetic field configurations applied in VTF. In (a) the poloidal field coils are located outside the vessel yielding an open cusp configuration where the field lines intersect the vacuum vessel walls. In (b) the closed cusp configuration is produced by in-vessel coils such that the field lines are confined in the experiment.

3.1 Experiments in the VTF open configuration

In the open cusp configuration the plasma is produced by 20kW of 2.45GHz RF radiation. The applied RF heating breaks down the neutral gas (typically hydrogen or argon) at the

resonance location ($B = 87$ mT) where the electron cyclotron frequency matches the heating frequency. For the hydrogen discharges forming the basis for the data in Fig. 2(a,b) the toroidal magnetic field is adjusted such that the resonances location is a cylindrical surface with a radius of 1 m. The number density is about $5 \cdot 10^{16}$ m^{-3} and the electron temperature is on the order of 20 eV yielding a mean-free path between electron-ion collisions (as well as electron-neutral collisions) larger than the dimensions of the experiment. The short pulse length ~ 10 ms allows us to measure the plasma and field properties using standard electrostatic and magnetic probe techniques [23, 24].

Reconnection is driven by energizing a central solenoid which induces a toroidal loop voltage (typically about 70 V). Given the large aspect-ratio of the experimental geometry this inductive/reconnection electric field is nearly uniform. The sequence of sub-figures in Fig 2(a) show the evolution of the plasma current contours as the external reconnection drive is energized. The dashed lines represent the experimentally inferred magnetic field lines; two field lines are highlighted such that their motion can be followed as they reconnect and drift apart.
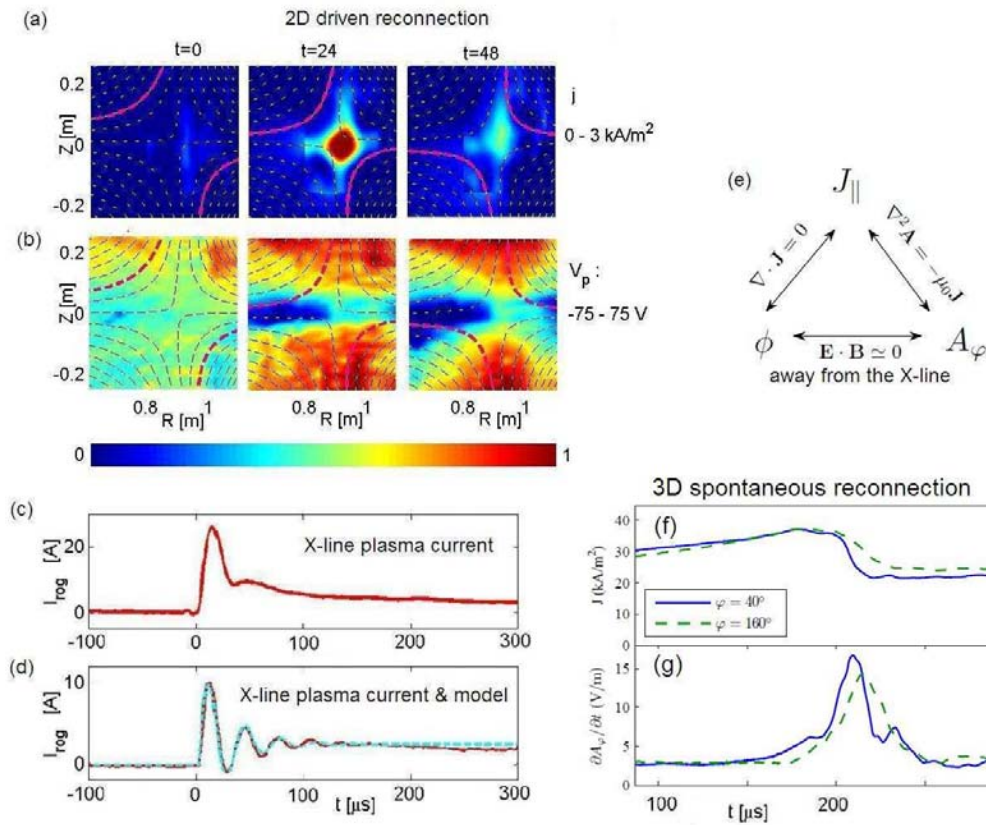

Figure 2: (a,b) Measured contours of plasma current, and electrostatic potential during the initial phase of the forced reconnection pulse. Each column of subfigures corresponds to a snapshot in time as indicated at the top. (c,d) Total current in the x-line region as measured by a Rogowski coil in an open cusp hydrogen and argon discharge respectively. (e) Set of equations which can account for the oscillatory response observed in 2D reconnection as well as the exponentially growing reconnection rate in 3D reconnection events. (f) Plasma current recorded as a function of time in the x-line region at two separate toroidal locations during a 3D reconnection event in the closed cusp configuration. (g) The reconnection electric field pulses corresponding to the behavior of the plasma current shown in (f).

4

3.2 Effects of electron trapping

In Fig. 2(c) the current measured by a Rogowski coil is shown as a function of time. This Rogowski coil measures the total current in an area 0.1×0.2 m^2 centered on the x-line. After the initial spike the x-line current is about 10 A, which is about 1000 times less than the current estimated when using classical Spitzer resistivity. The smallness of the experimental current has been explained by solving the Vlasov equation ($df/dt = 0$ along particle orbits) using the measured electric and magnetic field as input to a massively parallel orbit solver [25]. The analysis shows that in this open cusp the electrons are not free to go around toroidally because the field lines intersect the vacuum vessel wall. Rather they are bound to *trapped* trajectories continuously bouncing back and forth along a given field line. On a slower time scale (controlled by the external reconnection drive) the field lines convect through the reconnection region carrying the trapped electrons along. As the trapped electrons convect across the x-line region they take a finite step in the toroidal direction. This step size is controlled by the ratio of the guide field and the in-plane field, $B_{\mathrm{guide}}/\nabla B_{\mathrm{cusp}}$. Furthermore, the flux of electrons across the layer is proportional to nE_{rec} yielding a scaling consistent with the experimental observations

$$j_{\parallel} \propto nE_{\mathrm{rec}}B_{\mathrm{guide}}/\nabla B_{\mathrm{cusp}} \quad . \tag{1}$$

The described trapping can occur inside the bulk of the plasma where the electrons may bounce due to electrical forces or the magnetic mirror force. Meanwhile, the sheath potentials at the interface with the vacuum vessel walls that render the trapping nearly perfect; the electrons will only "leak" out to the walls at a slower time scale controlled by the ions, such that the plasma remains quasi neutral.

3.3 The generic role of electron trapping in collisionless reconnection

The role of the walls in trapping the electrons in the experiment suggests that trapping may not be important in more generic reconnection scenarios. However, analysis of electron distribution functions measured near reconnection regions in the Earth's magnetotail show that strong parallel electric fields develop self-consistently and traps nearly all thermal electrons [1, 26]. As a result the electron dynamics in magnetotail reconnection become similar to that observed in the experiment. A new adiabatic model for the electrons has been derived providing a simple analytical expression for $f(v_{\parallel}, v_{\perp})$ which includes the nonlinear effects of magnetic and electrical trapping [27]. This model formed the basis for the derivation of the anisotropic equations of state yielding the parallel and perpendicular pressures as a function of the plasma density and magnetic field strength [28]. In the low density limit the equations of state coincide with the Boltzman response $p_{\parallel} = p_{\perp} = nT$, whereas in the high density limit (where nearly all electrons are trapped) the equations resemble the CGL scalings [29] with $p_{\parallel} \propto n^3/B^2$ and $p_{\perp} \propto nB$. The new equations of state have been confirmed in fully kinetic simulations of reconnection where it is found that they control the inner structure of the reconnection region [30]. The parallel electric fields which are responsible for trapping become substantial in configurations where $\beta_e = 2\mu_0 p_e/B^2$ (the electron pressure normalized to the magnetic field pressure) is small in the upstream inflow region, $\beta_{e\infty} \leq 0.01$. As such, in the Earth magnetotail (where $\beta_{e\infty}$ can be small [26]) it is likely that the parallel electric fields play a major role in the energization of the observed super-thermal electrons [31].

3.4 Dynamical plasma response in 2D reconnection

We now focus on the temporal variation of the plasma current as summarized in Figs. 2(c,d). The trace in Fig. 2(c) is for the hydrogen discharge of Fig. 2(a,b), whereas the response shown by the red line in Fig. 2(d) is recorded in an argon discharge with a stronger in-plane magnetic field but otherwise similar to the hydrogen discharge. The dashed light-blue line is obtained with a simple model which we will summarize below; later this model will aid our understanding of the 3D spontaneous reconnection dynamics observed in the closed magnetic configuration.

The model for the oscillatory response is based on the triangle of equations shown in Fig. 2(e). Consistent with the observations, in the model we assume that the various quantities, $Q(\mathbf{x}, t)$ can be approximated by the form $Q(\mathbf{x}, t) \simeq Q_x(\mathbf{x}) Q_t(t)$ such that the spatial and temporal response is separable. The link between the in-plane potential ϕ and the toroidal component of the magnetic vector potential A_φ was documented in Ref. [32]. The potential develops in order to maintain $\mathbf{E} \cdot \mathbf{B} \simeq 0$ away from the x-line. This condition follows directly from our expectation that the plasma in the inflow and exhaust regions should approximately be ideal, $\mathbf{E} + \mathbf{v} \times \mathbf{B} \simeq 0$. Given the plasma current is much smaller than the current applied in the poloidal field coils, the magnetic geometry is dominated by the vacuum magnetic field of these coils. Furthermore, the reconnection electric field $E_{\text{rec}} = -\partial A_\varphi / \partial t$ is nearly uniform across the experimental cross-section and often dominated by that induced by the external, central solenoid. Thus, the only freedom that the plasma has to maintain $\mathbf{E} \cdot \mathbf{B} \simeq E_{\text{rec}} B_{\text{guide}} - \nabla \phi \cdot \mathbf{B}_{\text{cusp}} \simeq 0$ away from the x-line, is to develop an appropriate in-plane potential, ϕ. Experimentally we have verified that ϕ is proportional to $E_{\text{rec}} = -\partial A_\varphi / \partial t$ and that it reduces the region where $\mathbf{E} \cdot \mathbf{B}$ is large to an area of about 5 cm $\times$ 5 cm centered on the x-line [33]. The spatial from of ϕ seen in Fig. 2(b) is typical and its temporal evolution is governed by

$$\phi = -\alpha_1 \frac{\partial A_\varphi}{\partial t} \ , \quad \alpha_1 > 0 \ , \tag{2}$$

where α_1 is a positive constant related to the ratio of $B_{\text{guide}}/B_{\text{cusp}}$ and the geometry of the experiment. Note that in the strong guide field regime the E$\times$B-flow of the electrons is given by $v_{\text{ExB}} \simeq -\nabla \phi \times \mathbf{B}_\phi / B^2$. Thus, ϕ is the electron flow function where the flow is along contours for constant ϕ.

Next, in the triangle of Fig. 2(e) the relationship between the A_φ and $j_\parallel$ simply follows from Biot-Savart's law $A_\varphi = (\mu_0/4\pi) \int j_\parallel / |\mathbf{x}' - \mathbf{x}| \, d^3 x' + A_{\text{ext}}$. Experimentally, we find that A_φ is nearly uniform over the cross-section. Furthermore, while the current profile changes in time its spatial profile remains nearly constant permitting a simple expression for its scalar strength,

$$A_\varphi = \alpha_2 j_\parallel + A_{\text{ext}} \ , \quad \alpha_2 > 0 \quad . \tag{3}$$

We finally consider the last equation on the triangle in Fig. 2(e) where the condition of quasi-neutrality requires $\nabla \cdot \mathbf{j} = 0$ and relates ϕ to $j_\parallel$. More specifically, when ϕ increases, perpendicular ion polarization currents are driven $\mathbf{j}_p = -(nm_i/B^2)\nabla \partial \phi / \partial t$ which, as shown in Fig. 3(a), point away from the vertical separator and towards the horizontal separator. For the plasma to remain quasi-neutral parallel electron currents flow along the field lines. Because of the strong guide magnetic field the parallel electron currents,

$j_\parallel = n m_i / B^2 \int_{\text{edge}}^{\mathbf{x}} \nabla_\perp^2 \partial\phi / \partial t \, dl$ are mostly toroidal (here the dl is along field lines). By fitting an analytical expression to the experimental ϕ a theoretical profile for $j_\parallel$ is obtained, which is in good agreement with that observed in the experiment (see Fig. 3(b,c)) [33, 34]. For the scalar amplitude of the current we thus obtain an expression of the form

$$j_\parallel = \alpha_3 \frac{\partial\phi}{\partial t} \quad , \qquad \alpha_3 > 0 \quad . \tag{4}$$

This current is different in nature from that in Eq. (1) driven by the reconnection electric field. The current described in Eq. (4) is caused by simple shifts in the center location of the electrons bounce orbits in their rapid motion back and forth along field lines.

By combining Eqs. (2), (3), and (4) we obtain a single second order differential equation

$$A_\varphi = -\alpha \frac{\partial^2 A_\varphi}{\partial t^2} + A_{\text{ext}} \quad , \qquad \alpha = \alpha_1 \alpha_2 \alpha_3 > 0 \quad . \tag{5}$$

In this equation the positive constant α can be determined accurately from the plasma measurements and the experimental geometry. When including damping due to the dissipative current in Eq. (1) the solutions of Eq. (5) are in excellent agreement with the experimental observations. The model has been verified for a large set of experimental parameters yielding a range of oscillation frequencies $\omega = \sqrt{1/\alpha}$ [34]. Again, an example of the match between the model and experiment is shown in Fig. 2(d).
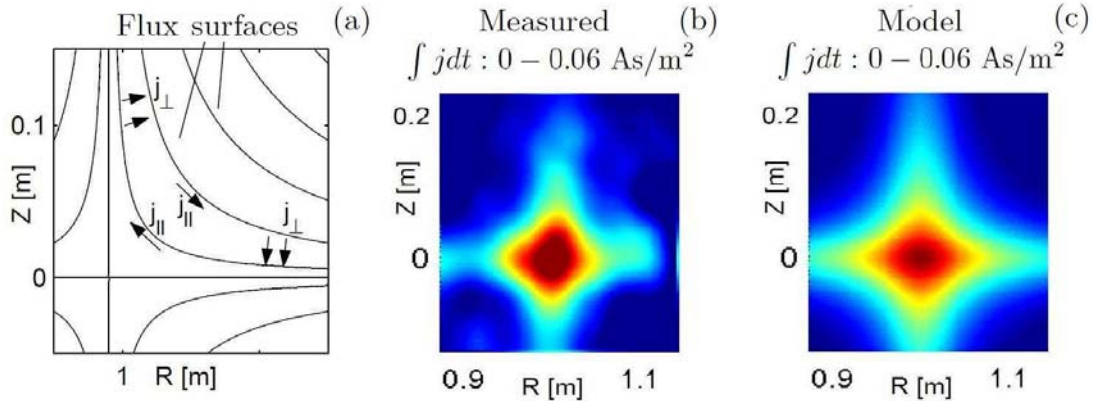

Figure 3: (a) Illustration of the system of currents driven by time variations in ϕ. The ion-polarization currents $j_\perp$ and field-aligned electron currents form closed current loops. (b,c) Experimental and theoretical toroidal current profiles driven by changes in ϕ.

4   Experimental observations of 3D spontaneous reconnection

We now turn to the experimental results of the VTF closed magnetic cusp configuration shown in Fig. 1(b). Here the in-plane magnetic field is produced by internal coils and the resulting geometry allows electrons to stream freely in the toroidal direction without significant trapping effects. A target plasma is established by 1 ms ohmic heating of an RF

seed plasma. In typical argon discharges the electron temperature reaches about 25 eV and the density is on the order of 10^{18} m^{-3}. The temperature of the ions is not known but is assumed to be much colder than the electron temperature. Although the plasma parameters are very different in this configuration, we will describe below how the theoretical framework applied to the open configuration can be amended to account for the onset phase of the 3D reconnection events.

Reconnection is driven by manipulating the current in the four internal coils. Often the observed reconnection rate is slow because a current sheet builds which effectively stores the applied magnetic stress. However, a range of experimental parameters exist were sudden bursts of 3D reconnection are observed as the current sheet rapidly breaks up [2]. An example is given in Fig. 2(f) where the current density is shown as a function of time for two separate cross-sections. We observe how the current density rapidly falls off at the toroidal angle $\varphi = 40°$ about 10 μs before it decreases at $\varphi = 160°$. As seen in Fig. 2(g), these modifications in the plasma current are associated with the toroidally asymmetric pulses in $E_{\text{rec}} = -\partial A_\varphi/\partial t$, which we define as the reconnection rate.

As was the case for the open cusp experiment we model the onset of reconnection based on the triangle of equations shown in Fig. 2(e) and we assume again that the various quantities, $Q(\mathbf{x}, t)$ can be approximated by the form $Q(\mathbf{x}, t) \simeq Q_x(\mathbf{x})Q_t(t)$. This allows us to understand the initial dynamics and growth in the reconnection rate corresponding to a time up to $t \simeq 200\mu$s in Figs. 2(f,g). After this time the effects of saturation and reconnection propagating around the torus become important. Those effects are not covered by the present analysis.
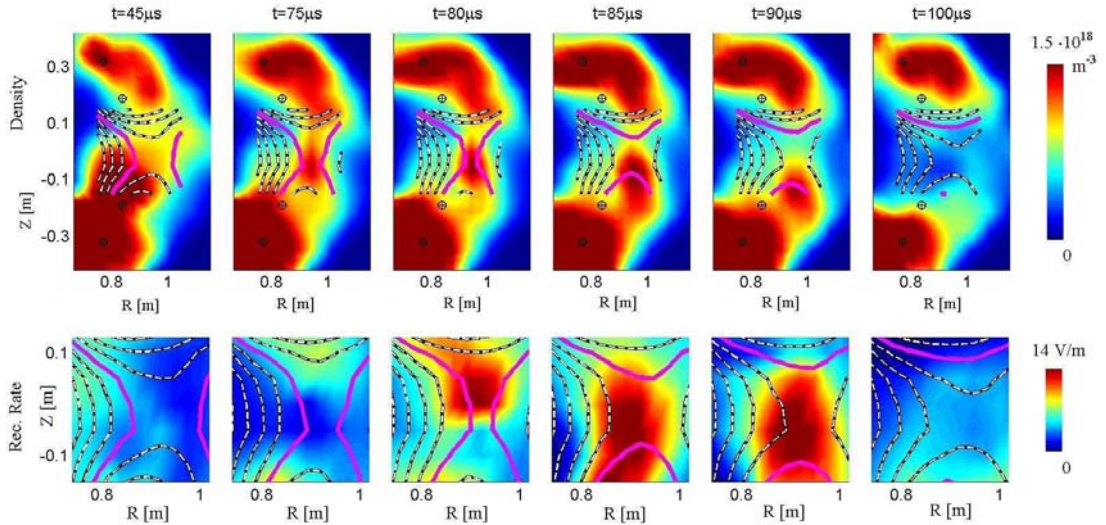

Figure 4: Measured contours of the plasma density and the reconnection rate. The measurements were obtained in a 55 μs time interval centered about a spontaneous reconnection event.

The details of the 3D reconnection events are studied using about 1250 magnetic and electrostatic probes digitized simultaneously at 2MHz. For example, the bottom row in Fig. 4 shows the measured contours of $-\partial A_\varphi/\partial t$ during a 55 μs period centered on the reconnection event. The dashed lines are the magnetic field lines which coincide with contours of constant RA_φ. In the first two time slices the reconnection region is becoming increasingly stretched. Then, for a time interval of about 15 μs the reconnection rate jumps well above

15 V/m. In this time interval the highlighted set of field lines merge, reconnect and drift apart while the magnetic stress in the system is greatly reduced.

In the top row of Fig. 4 the measured field lines are superimposed on contours of measured plasma density. During the reconnection event it is seen that the central density is ejected downwards at a velocity consistent with the motion of the highlighted magnetic field lines. A more detailed analysis shows that the plasma moves downwards at about 10 km/s, corresponding to the Alfvén speed calculated with the in-plane magnetic field [2].
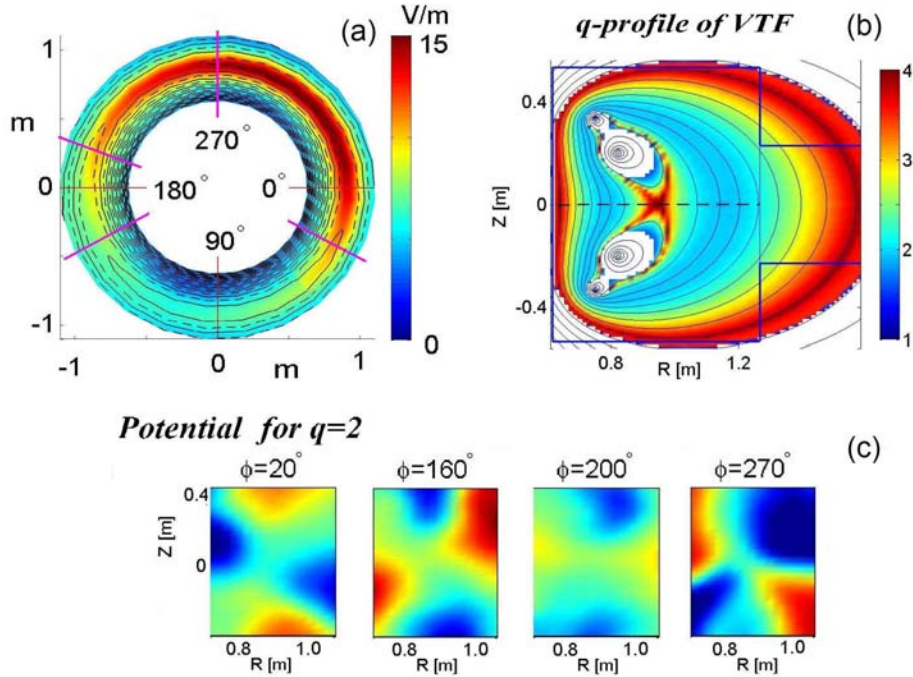

Figure 5: (a) Inductive (reconnection) electric field measured at the mid-plane of the VTF at the onset of spontaneous reconnection. (b) q-profile for a typical VTF discharge; $q \simeq 2$ in the shared flux region yields spontaneous reconnection events. (c) Electrostatic in-plane potential measured at various toroidal cross-sections (as indicated by the red lines in (a)). In the region where $q \simeq 2$ the potential rotates with the magnetic field lines.

The 3D nature of the events becomes more clear in Fig. 5(a) where the reconnection electric field is shown as measured at the horizontal mid-plane of VTF at the time of the onset. For this particular shot the reconnection starts close to $\varphi = 270°$. We find that the spontaneous reconnection events are closely tied to the tokamak safety factor q, which is the number of times a field line goes around toroidally for one poloidal circuit. A typical q-profile is given in Fig. 5(b). This profile can be scaled by adjusting the strength of the toroidal magnetic field. Reconnection pulses are only observed for rational values, $q \simeq 2$ or $q \simeq 3$, in the shared flux region where the field lines circulate all for conductors.

When q is rational in the shared flux region a mode is permitted which develops in conjunction with the burst of reconnection. Fig. 5(c) documents the mode potential observed at four separate toroidal cross-sections at the time of the reconnection onset; the mode structure follows the field line rotation of the $q \simeq 2$ magnetic geometry considered. Compared to the open cusp, the separators of the closed cusp configuration are rotated by 45° counter clockwise (compare Fig. 1(a,b)). Taking this rotation in account, at the toroidal angle of
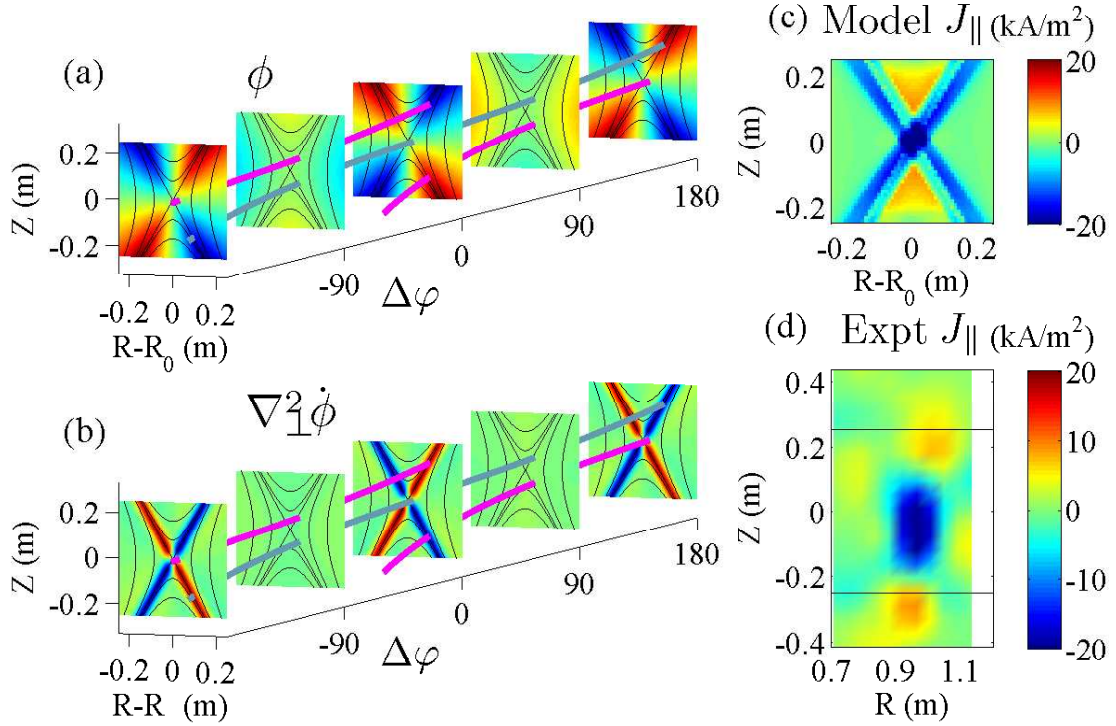
Figure 6: (a) Potential model, ϕ fitted from experimental data with the gray magnetic-field line, which passes by the x-line near the onset location ($\varphi = 0$); (b) divergence of ion polarization currents $\propto \nabla^2_\perp \partial\phi/\partial t$. c) experimentally measured change in $j_\parallel$ during the $8\mu s$ leading up to peak reconnection; (d) integration of (b) along field lines which gives an asymmetric parallel current similar to that experimentally observed.

the onset location ($\varphi = 270°$ in Fig. 5(a,c)) the in-plane potential, ϕ, has the same phase and form as ϕ observed in the open cusp and shown in Fig 2(b) at $t = 48\mu s$. Thus, at the onset angle, $\varphi \simeq 270°$, the potential helps reduce the area where $\mathbf{E} \cdot \mathbf{B}$ is finite (see the discussion for the open geometry), and although the structure of ϕ now is three dimensional we find that its scalar strength and E_{rec} are related as described in Eq. (2) for the open configuration.

Next, from Biot-Savart's law $A_\varphi = (\mu_0/4\pi) \int j_\parallel / |\mathbf{x}' - \mathbf{x}| \, d^3x'$ it follows that a local positive pulse in in $E_{\text{rec}} = -\partial A_\varphi/\partial t$ must be associated with a local decrease in the parallel current density. Therefore, the scalar strength of the three dimensional perturbations are still related by Eq. (3), where $\alpha_1 > 0$ can be calculated from the spatial structure of the parallel current perturbation $\Delta j_\parallel$.

The potential structure of Fig. 5(c) is essential for explaining current continuity and obtaining an approximation for $\Delta j_\parallel$. The asymmetric $\partial A_\varphi/\partial t$ implies that the field-aligned current at the x-line no longer closes in toroidal loops. Since quasi neutrality requires $\nabla_\parallel j_\parallel + \nabla_\perp \cdot \mathbf{j}_\perp = 0$ there must be perpendicular currents that compensate for the asymmetry. These are again ion polarization currents, controlled by ϕ. To quantify this effect as illustrated in Fig. 6 we consider a toroidal volume with a 0.4 m × 0.4 m poloidal cross

section. For this volume, we can write the asymmetric part of the parallel current as

$$\Delta j_\parallel(\mathbf{x}) = j_{\text{edge}} + \int_{\text{edge}}^{\mathbf{x}} \frac{nm_i}{B^2} \nabla_\perp^2 \frac{\partial \phi}{\partial t} dl \quad , \tag{6}$$

where the integral is evaluated along field lines with n uniform. j_{edge} is assumed to be evenly distributed between the two locations where each field line reaches the edge of the toroidal volume considered. To evaluate Eq. (6) we use model fields chosen to match the experimental profiles. As an example, the rotating potential is approximated as shown in Fig. 6(a) yielding a 3D structure in $\nabla_\perp^2 \phi$ as shown in Fig. 6(b). After evaluating the integral in Eq. (6) we obtain $\Delta j_\parallel$; in Figs. 6(c,d) the model and experimental $\Delta j_\parallel$ are compared at the toroidal cross-section of the onset. It is seen that our model captures the key physics to correctly describe the toroidally localized decrease in the parallel current. Due to the mapping of the field lines, the current perturbation at the onset location is related to $\nabla_\perp^2 \phi$ throughout the entire experiment. In contrast to the 2D case, we find for the rotating ϕ of the 3D events that $\Delta j_\parallel$ is negative near the x-line. Thus, Eq. (4) of the 2D case has to be modified by a minus sign:

$$j_\parallel = -\alpha_3 \frac{\partial \phi}{\partial t} \quad , \qquad \alpha_3 > 0 \quad . \tag{7}$$

We have now established the relationships between ϕ, A_φ and $j_\parallel$ as outlined in Fig. 2(e) also for the 3D reconnection events. By combining Eqs. (2), (3) and (7) we obtain

$$A_\varphi = \alpha \frac{\partial^2 A_\varphi}{\partial t^2} + A_{\text{ext}} \quad , \qquad \alpha = \alpha_1 \alpha_2 \alpha_3 > 0 \quad . \tag{8}$$

Because of the change in sign in the parallel currents driven by the 3D structure of ϕ, we now have exponentially growing solutions. The numerical value of the model growth rate $\gamma = \sqrt{1/\alpha} \sim 20~\mu$s was determined by Katz, et al. [35] and is in excellent agreement with that experimentally observed.

5 Discussion and Conclusions

In this report we have provided an overview of the experimental results on reconnection in VTF. We find that a common theoretical framework can account for the oscillatory re-connection response of the VTF open configuration as well as the spontaneous reconnec-tion events in the VTF closed configuration. We identify that the key physics causing the spontaneous onset of reconnection is the interaction between the reconnection x-line and a global mode which is permitted for rational q in the closed configuration. We have docu-mented details of spontaneous events observed for $q \simeq 2$, but we also observe events where $q \simeq 3$. The key physics that allow for spontaneous reconnection is the breaking of toroidal symmetry caused by the global mode.

Both for 2D and 3D reconnection we find that strong ion-polarization currents are driven by the changing in-plane potential. In turn, these perpendicular ion currents drive parallel

electron currents to maintain quasi neutrality. In the open cusp scenario, where reconnection remains 2D, we established a second order differential equation which can account for the oscillatory behavior. The model was based on the links between 1) the reconnection rate and the in-plane potential, 2) the in-plane potential and the parallel electron currents and 3) by the parallel electron currents and the inductive reconnection electric field. For the 2D events these links (or constraints) yield a second order differential equations with oscillatory solutions.

For the 3D events we obtain a similar set of relationships. However, the global mode, manifested in a strong in-plane potential rotating with the magnetic field lines outside the reconnection region, breaks the axisymmetry and causes a change in sign of the parallel electron currents driven by the time varying in-plane potential. Incorporating this, we find a second order differential equation which has exponentially growing solutions and predicts growth rate consistent with those experimentally observed.

Our relatively crude analysis is guided and validated by the detailed experimental data which permitted us to approximate the spatial and temporal variations in plasma and field quantities by expressions on the form $Q(t, \mathbf{x}) \simeq Q_t(t) Q_x(\mathbf{x})$. It is important to note that the the success of this formalism for the 3D events may be seen as consequence of strong "mode locking". The 3D events clearly include the interaction between perturbations near the x-line with $(m, n) = (0, 1)$ and external perturbations with $(m, n) = (2, 1)$. Here m and n are the poloidal and toroidal mode numbers, respectively. Also higher order modes will be necessary to account for the details of the experimental profiles. This makes our observations relevant to the results of MST [19], where large spontaneous events include mode locking between modes with a range of different m and n numbers. Similar dynamics also appear to be important in recent observations of sawtooth reconnection [22] where higher order modes are observed before and after the reconnection events.

References

[1] J. Egedal, M. Øieroset, W. Fox, and Lin R. P. In situ discovery of an electrostatic potential, trapping electrons and mediating fast reconnection in the earth's magnetotail. *Phys. Rev. Lett.*, 94(2):025006, JAN 21 2005.

[2] J. Egedal, W. Fox, N. Katz, M. Porkolab, K. Reim, and E. Zhang. Laboratory observations of spontaneous magnetic reconnection. *Phys. Rev. Lett.*, 98(1):015003, JAN 5 2007.

[3] J. Dungey. Conditions for the occurence of electrical discharges in astrophysical systems. *Philosophical Magazine*, 44:725, 1953.

[4] J. B. Taylor. Relaxation and magnetic reconnection in plasmas. *Reviews of Modern Physics*, 58(3):741–763, JUL 1986.

[5] V. M. Vasyliunas. Theoretical models of magnetic-field line merging .1. *Reviews of Geophysics*, 13(1):303–336, 1975.

[6] T. D. Phan, L. M. Kistler, B. Klecker, G. Haerendel, G. Paschmann, B. U. O. Sonnerup, W. Baumjohann, M. B. Bavassano-Cattaneo, C. W. Carlson, A. M. Dilellis, K. H. Fornacon, L. A. Frank, M. Fujimoto, E. Georgescu, S. Kokubun, E. Moebius, T. Mukai, M. Øieroset, W. R. Paterson, and H. Reme. Extended magnetic reconnection at the earth's magnetopause from detection of bi-directional jets. *Nature*, 404(6780):848–850, APR 20 2000.

[7] S. Masuda, T. Kosugi, H. Hara, and Y. Ogawaray. A loop top hard x-reay source i a compact solar-flare as evidence for magnetic reconnection. *Nature*, 371(6497):495–497, OCT 6 1994.

[8] R. J. Hastie. Sawtooth instability in tokamak plasmas. *Astrophysics and Space Science*, 256(1-2):177–204, 1998.

[9] H. K. Park, N. C. Luhmann, A. J. H. Donne, I. G. J. Classen, C. W. Domier, E. Mazzucato, T. Munsat, M. J. V. de Pol, Z. Xia, and TEXTOR team. Observation of high-field-side crash and heat transfer during sawtooth oscillation in magnetically confined plasmas. *Phys. Rev. Lett.*, 96(19):195003, MAY 19 2006.

[10] B. U. O Sonnerup. *Magnetic field reconnection, in Solar System Plasma Physics, vol. 3.* edited by L. T. Lanzerotti, C. F. Kennel, and E. N. Parker, pp. 45 108, North-Holland, New York, 1979.

[11] J. Birn, J. F. Drake, M. A. Shay, B. N. Rogers, R. E. Denton, M. Hesse, M. Kuznetsova, Z. W. Ma, A. Bhattacharjee, A. Otto, and P. L. Pritchett. Geospace environmental modeling (GEM) magnetic reconnection challenge. *J. Geophys. Res.*, 106(A3):3715–3719, MAR 1 2001.

[12] Y. Ren, M. Yamada, S. Gerhardt, H. T. Ji, R. Kulsrud, and A. Kuritsyn. Experimental verification of the hall effect during magnetic reconnection in a laboratory plasma. *Phys. Rev. Lett.*, 95(5):055003, JUL 29 2005.

[13] X. G. Wang and A. Bhattacharjee. Nonlinear dynamics of the m = 1 instability and fast sawtooth collapse in high-temperature plasmas. *Phys. Rev. Lett.*, 70(11):1627–1630, MAR 15 1993.

[14] A. Bhattacharjee, K. Germaschewski, and C. S. Ng. Current singularities: Drivers of impulsive reconnection. *Phys. Plasmas*, 12(4):042305, APR 2005.

[15] P. L. Pritchett. Onset and saturation of guide-field magnetic reconnection. *Phys. Plasmas*, 12(6):062301, JUN 2005.

[16] P. A. Cassak, M. A. Shay, and J. F. Drake. Catastrophe model for fast magnetic reconnection onset. *Phys. Rev. Lett.*, 95(23):235002, DEC 2 2005.

[17] L. Li and J. Zhang. On the brightening propagation of post-flare loops observed by trace. *The Astrophysical Journal*, 690(1):347–357, 2009.

[18] D. Tripathi, H. Isobe, and H. E. Mason. On the propagation of brightening after filament/prominence eruptions, as seen by soho-eit. *Astronomy and Astrophysics*, 453(3):1111–1116, July 2006.

[19] S. Choi, D. Craig, F. Ebrahimi, and S. C. Prager. Cause of sudden magnetic reconnection in a laboratory plasma. *Phys. Rev. Lett.*, 96(14):145004, APR 14 2006.

[20] H. K. Park, A. J. H. Donné, Jr, I. G. J. Classen, C. W. Domier, E. Mazzucato, T. Munsat, M. J. van de Pol, and Xia. Comparison study of 2d images of temperature fluctuations during sawtooth oscillation with theoretical models. *Physical Review Letters*, 96(19):195004, 2006.

[21] H. K. Park, E. Mazzucato, Jr, C. W. Domier, Z. Xia, T. Munsat, A. J. H. Donné, I. G. J. Classen, M. J. van de Pol, and Textor Team. Self-organized t_e redistribution during driven reconnection processes in high-temperature plasmas. *Physics of Plasmas*, 13(5):055907+, 2006.

[22] T. Munsat, H. K. Park, I. G. J. Classen, C. W. Domier, A. J. H. Donne, N. C. Luhmann, E. Mazzucato, and M. J. van de Pol. Localization of the magnetic reconnection zone during sawtooth crashes in tokamak plasmas. *Nuclear Fusion*, 47(11):L31–L35, NOV 2007.

[23] J. Egedal, A. Fasoli, M. Porkolab, and D. Tarkowski. Plasma generation and confinement in a toroidal magnetic cusp. *Review of Scientific Instruments*, 71(9):3351–3361, SEP 2000.

[24] A. Kesich, J. Bonde, J. Egedal, et al. Magnetic flux array for spontaneous magnetic reconnection experiments. *Review of Scientific Instruments*, 79, 2008.

[25] J. Egedal, W. Fox, E. Belonohy, and M. Porkolab. Kinetic simulation of the vtf magnetic reconnection experiment. *Computer Physics Communications*, 164(1-3):29–33, DEC 1 2004.

[26] J. Egedal, A. Le, N. Katz, L. J. Chen, B. Lefebvre, W. Daughton, and A. Fazakerley. Cluster observations of bidirectional beams caused by electron trapping during antiparallel reconnection. *J. Geophys. Res.*, 115, MAR 23 2010.

[27] J. Egedal, W. Fox, N. Katz, M. Porkolab, M. Øieroset, R. P. Lin, W. Daughton, and Drake J. F. Evidence and theory for trapped electrons in guide field magnetotail reconnection. *J. Geophys. Res.*, 113(6):A12207, MAR 25 2008.

[28] A. Le, J. Egedal, W. Daughton, W. Fox, and N. Katz. Equations of State for Collisionless Guide-Field Reconnection. *Phys. Rev. Lett.*, 102(8), FEB 27 2009.

[29] G. F. Chew, M. L. Goldberger, and F. E. Low. The boltzmann equation and the one-fluid hydromagnetic equations in the absence of particle collisions. *Proc. Royal Soc. A*, 112:236, 1956.

[30] A. Le, J. Egedal, W. Daughton, J. F. Drake, W. Fox, and N. Katz. Magnitude of the Hall fields during magnetic reconnection. *Geophy. Res. Lett.*, 37, FEB 11 2010.

[31] J. Egedal, A. Le, Y. Zhu, W. Daughton, M. Øieroset, T. Phan, R. P. Lin, and J. P. Eastwood. Cause of super-thermal electron heating during magnetotail reconnection. *Geophy. Res. Lett.*, 37, MAY 28 2010.

[32] J. Egedal and A. Fasoli. Single-particle dynamics in collisionless magnetic reconnection. *Phys. Rev. Lett.*, 86(22):5047–5050, MAY 28 2001.

[33] J. Egedal, A. Fasoli, and J. Nazemi. Dynamical plasma response during driven magnetic reconnection. *Phys. Rev. Lett.*, 90(13):135003, APR 4 2003.

[34] J. Egedal, W. Fox, M. Porkolab, and A. Fasoli. Eigenmode response to driven magnetic reconnection in a collisionless plasma. *Phys. Plasmas*, 12(5):052107, MAY 2005.

[35] N. Katz, J. Egedal, W. Fox, A. Le, J. Bonde, and A. Vrublevskis. Laboratory observation of localized onset of magnetic reconnection. *Phys. Rev. Lett.*, 104(25), JUN 25 2010.

Unified model for experimental observations of 2D and 3D magnetic reconnection

(a) 2D driven reconnection
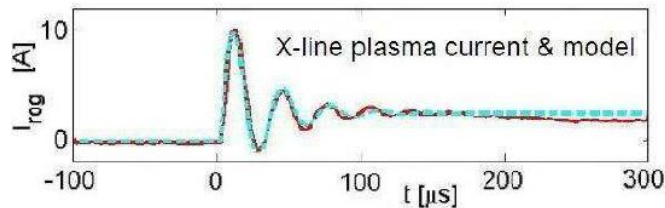
(b) 3D spontaneous reconnection
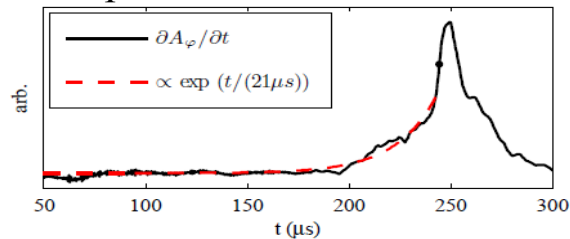
(a) Oscillatory plasma current observed in steadily driven 2D reconnection. The dynamic behavior is well described in a simple model based on Maxwell's equations and the requirement of current continuity.

(b) Recorded reconnection rate during the onset of spontaneous of reconnection. The model derived of 2D reconnection is generalized to 3D and accurately account for the exponential growth in the reconnection rate.

.

Magnetic reconnection is studied in the collisionless limit at the Versatile Toroidal Facility (VTF) at MIT. Two distinct magnetic configurations are applied in the experiments; an open magnetic cusp and a closed cusp. In the open cusp configurations the field lines intersect the vacuum vessel walls and here axisymmetric oscillatory reconnection is observed.

In the closed cusp configuration, where the field lines are confined inside the experiment, the coupling between global modes and a current sheet leads to powerful bursts of 3D spontaneous reconnection [1]. These spontaneous events start at one toroidal location, and then propagate around the toroidal direction at the Alfven speed (calculated with the strength of the dominant guide field). The three dimensional measurements include the detailed time evolution of the plasma density, current density, the magnetic flux function, the electrostatic potential, and the reconnection rate [2].

The vastly different plasma behavior in the two configurations can be described using a simple theoretical framework, linking together the interdependencies of the reconnection rate, the in-plane electrostatic potential and the parallel electron currents. We find that it is the breaking of toroidal symmetry by the global mode that allows for a localized disruption of the x-line current and hereby facilitates the onset of spontaneous reconnection [3]
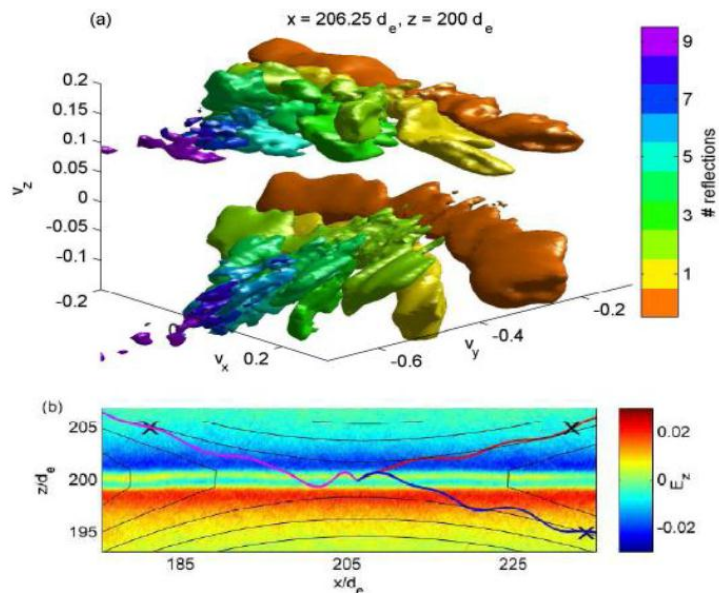
[1] Egedal J, et al., (2007) Phys. Rev. Lett. 98, 015003.
[2] Katz N, et al., (2010) Phys. Rev. Lett. 104, 255004.
[3] Egedal J, et al., (2011) Phys. Plasmas, submitted.

The structure of the electron phase-space distribution during anti-parallel reconnection

(a) Isosurface of the reconstructed electron distribution at the x-line in a PIC simulation. The different colors correspond to the number of times electrons have been reflected in the diffusion region (b) Electron orbits reaching the x line with 0, 1 and 2 reflections. Color plot is in-plane electric field *Ez*, with contours of in-plane projection of the magnetic field lines.

Observations in the Earth's magnetotail and kinetic simulations of magnetic reconnection have shown high electron pressure and temperature anisotropy in the inflow of the electron diffusion region. This anisotropy is accurately accounted for in a new fluid closure for collisionless reconnection [1], and we find that the anisotropy drives the electron current in the diffusion region, which is insensitive to the reconnection electric field.

By tracing electron orbits in the fields taken from particle-in-cell simulations [2], we reconstruct the electron distribution function in the diffusion region at enhanced resolutions, revealing its highly structured nature, with striations corresponding to the number of times an electron has been reflected within the region (see Fig.). The analysis reveals how the upstream electron anisotropy drives the current in the layer independent of the reconnection electric field. In turn, the analysis also exposes the origin of gradients in the electron pressure tensor important for momentum balance in the region and the mechanism by which the anisotropy sets the structure of the region [3].

[1] Le A, Egedal J, et al., Phys. Plasmas 17, 055703 (2010).
[2] Daughton W, et al. Phys. Plasmas 13, 072101 (2006).
[3] Ng J, Egedal J, et al., Phys. Rev. Lett. 106, 065002 (2011).